

Spectrum of Supernova Neutrinos in Ultra-pure Scintillators

C. Lujan-Peschard,^{a,b} G. Pagliaroli,^a F. Vissani.^{a,c}

^aLaboratori Nazionali del Gran Sasso, INFN, Assergi (AQ), Italy

^bDepartamento de Física, DCEI, Universidad de Guanajuato, León, Guanajuato, México

^cGran Sasso Science Institute, INFN, L'Aquila (AQ), Italy

E-mail: carolup@fisica.ugto.mx, giulia.pagliaroli@lngs.infn.it,
francesco.vissani@lngs.infn.it

Abstract. There is a great interest in measuring the non-electronic component of neutrinos from core collapse supernovae by observing, for the first time, also neutral-current reactions. In order to assess the physics potential of the ultra-pure scintillators in this respect, we study the entire expected energy spectrum in the Borexino, KamLAND and SNO+ detectors. We examine the various sources of uncertainties in the expectations, and in particular, those due to specific detector features and to the relevant cross sections. We discuss the possibility to identify the different neutrino flavors, and we quantify the effect of confusion, due to other components of the energy spectrum, overlapped with the neutral-current reactions of interest.

Contents

1	Introduction	1
2	Emission from a Standard Core Collapse Supernova	1
3	Interaction Channels	3
4	Description of the Ultra-pure Scintillating Detectors	5
5	Results	6
6	Conclusions	10

1 Introduction

A Core Collapse Supernova (SN) releases 99% of its total energy by emitting neutrinos of the six flavors. The capability to observe the electronic antineutrino component of this emission has already been proven by the detection of SN1987A neutrinos [1–3]. The very large statistics that we will collect from the next galactic supernova will allow us to study the time dependence of the spectrum, specific features of the $\bar{\nu}_e$ luminosity and of its average energy [4, 5]. The detection of the other neutrinos flavors, however, requires specific detectors and interactions, typically with smaller cross sections. This is true, in particular, for the non electronic component of the spectrum, that can be observed only through Neutral Current (NC) interactions.

During the last years a new generation of ultra-pure liquid scintillators, Borexino (BRX) [6] and KamLAND (KAM) [7], have been operated, obtaining excellent results thanks to the unprecedented low background levels reached and the new sensitivity in the very low energy range, below 1 MeV. They have a particularly good physics potential for the detection supernova NC channels, and quite remarkably, the Elastic Scattering (ES) of (anti)neutrinos on protons [8]. It has been argued that the high statistics from this reaction should suffice to constrain the spectra of the non electronic component for a SN emission, already with the existing detectors [9]. In view of the importance of this conclusion, we would like to reconsider it in this work.

The outline of this paper is as follows. First of all, we summarize the available information regarding SN neutrino detection in the existing ultra-pure scintillators, and calculate for each of them the total number of expected events as well as their spectral features. We consider the contributions of all neutrino interaction channels and obtain in this way the spectrum of events for a galactic supernova. In this way, we are in the position to evaluate which are the capabilities of the present generation of ultra-pure scintillators to identify and measure the different neutrino flavors.

2 Emission from a Standard Core Collapse Supernova

The aim of this work is to discuss an important question: what we can really see with the existing ultra-pure scintillators and to which extent we can distinguish the different neutrino

flavors. With this purpose in mind, we will use very conservative assumptions on the emission model. We suppose that the energy radiated in neutrinos is $\mathcal{E} = 3 \times 10^{53}$ erg, which is a typical theoretical value that does not contradict what is found in the most complete analyses of SN1987A events [10, 11]. We also assume that the energy is partitioned in equal amount among the six types of neutrinos, that should be true within a factor of 2 [12].

In agreement with the recent studies, e.g., [13], we consider quasi-thermal neutrinos, each species being characterized by an average energy $\langle E_i \rangle$ and including a mild deviation from a thermal distribution described by the parameter $\alpha = 3$ for all flavors. Thus, the neutrino fluence differential in the neutrino energy E is

$$\Phi_i = \frac{\mathcal{E}_i}{4\pi D^2} \times \frac{E^\alpha e^{-E/T_i}}{T_i^{\alpha+2} \Gamma(\alpha+2)} \quad i = \nu_e, \nu_\mu, \nu_\tau, \bar{\nu}_e, \bar{\nu}_\mu, \bar{\nu}_\tau$$

where the energy radiated in each specie is $\mathcal{E}_i = \mathcal{E} f_i$, with $f_i = 1/6$ in the case of equipartition, and the ‘temperature’ is $T_i = \langle E_i \rangle / (\alpha + 1)$. In particular, the neutrino and antineutrino fluences relevant to NC interactions

$$\Phi_\nu^{\text{SN}} = \Phi_{\nu_e} + 2\Phi_{\nu_\mu} \quad \text{and} \quad \Phi_{\bar{\nu}}^{\text{SN}} = \Phi_{\bar{\nu}_e} + 2\Phi_{\bar{\nu}_\mu}$$

since we suppose that the distribution of the 4 non-electronic species is identical.

The average energies are fixed by the following considerations: consistent with the simulations in [13] and with the findings from SN1987A [10, 11], we set the electron antineutrino average energy to $\langle E_{\bar{\nu}_e} \rangle = 12$ MeV. For the average energy of the non-electronic species, that cannot be seriously probed with SN1987A [11], we suppose that the non-electronic temperature is 30% higher than the one of $\bar{\nu}_e$: $\langle E_x \rangle = 15.6$ MeV, this is in the upper range of values, but still compatible with what is found in [12]. For a comparison we will consider also the worst case in which the energies of the non electronic component is equal to the one of the $\bar{\nu}_e$, namely $\langle E_x \rangle = 12$ MeV as showed in very recent simulation [14]. We calculate the electron neutrino average energy by the condition that the proton (or electron) fraction of the iron core in the neutron star forming is 0.4: this gives $\langle E_{\nu_e} \rangle = 9.5$ MeV.

Note that the NC reactions are independent from neutrino oscillations, while for the CC interactions also considering only the standard oscillation scenario, the choice of the mass hierarchy has an important impact on the expectations. Thanks to the fact that θ_{13} is large (say, larger than about 1 degree) this means that, in normal mass hierarchy, the survival probability of electron neutrinos and antineutrinos are $|U_{e3}^2|$ and $|U_{e1}^2|$ respectively, whereas for inverted mass hierarchy, the two values become $|U_{e2}^2|$ and $|U_{e3}^2|$. Thus, the approximate numerical values that we will assume in the calculations are

	$P_{\bar{\nu}_e \rightarrow \bar{\nu}_e}$	$P_{\nu_e \rightarrow \nu_e}$
Normal	0.7	0.0
Inverted	0.0	0.3

The value of $P_{\bar{\nu}_e \rightarrow \bar{\nu}_e}$ in the case of inverted hierachy means that what we measure as electronic antineutrinos in terrestrial detectors, are non-electronic antineutrinos at the emission in fact; thus, it has a particularly important impact on the interpretation of the data. We note also that these numerical values would imply that there are only little chances to probe the emission of electron neutrinos, which are, from the astrophysical point of view, the most important type of neutrinos emitted by a supernova.

In the following we will consider only the case of the normal mass hierarchy for definiteness and adding a bit of theoretical bias; recall however that this hypothesis is immaterial for

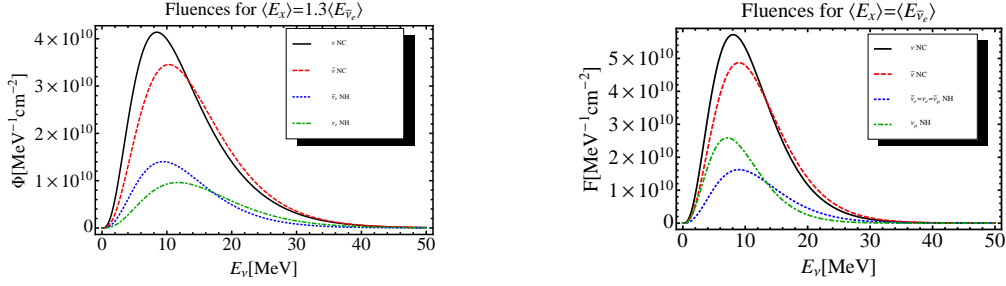


Figure 1. Fluences expected for the different neutrinos flavors. The blue dotted line shows $\bar{\nu}_e$, the green dot-dashed line ν_e . We assume standard neutrino oscillations and Normal mass Hierarchy (NH) for the fluences of each flavor. The black thick lines and the red dashed ones show the fluences relevant for the Neutral Current (NC) detection channels of neutrinos and antineutrinos, respectively.

the discussion of the neutral current events. The total fluences expected to reach the Earth under these assumptions are shown in Fig.1 for a Supernova exploding at 10 kpc from us.

3 Interaction Channels

In the scintillators and at SN energies, we need consider the several interaction processes:

CC processes. Those involving electronic antineutrinos are

- Inverse Beta Decay (IBD), i.e. $\bar{\nu}_e + p \rightarrow n + e^+$;
- $\bar{\nu}_e + {}^{12}\text{C} \rightarrow {}^{12}\text{B} + e^+$;

while those involving electronic neutrinos are

- Proton Knockout ${}^{12}\text{C}(\nu, pe^-){}^{11}\text{C}$;
- $\nu_e + {}^{12}\text{C} \rightarrow {}^{12}\text{N} + e^-$.

NC processes. We considered the following channels,

- ES on protons, $\bar{\nu} p \rightarrow \bar{\nu} p$;
- The 15.11 MeV de-excitation line of the ${}^{12}\text{C}$ nucleus, $\nu {}^{12}\text{C} \rightarrow \nu {}^{12}\text{C}^*$;
- The Proton Knockout $\bar{\nu} + {}^{12}\text{C} \rightarrow \bar{\nu} + {}^{11}\text{B}$.

Moreover, we consider the ES on electrons, that receives a contribution from both CC and NC. Let us discuss these reactions in detail.

Detailed description of the cross sections

The **IBD**, i.e., $\bar{\nu}_e + p \rightarrow n + e^+$, represents the main signal not only in water Cherenkov and also in scintillator detectors. It produces a continuous spectrum due to the positrons energy release. The approximated kinematic of this reaction connects the neutrinos energy with the detected energy through $E_\nu = E_d + Q - m_e$ where $Q \simeq 1.3$ MeV is the Q value of the reaction

and m_e is the electron mass. For the calculations, the IBD cross section reported in [15] was used. The **delayed neutron capture** on a proton is characterized by a monochromatic $\gamma_{2.2 \text{ MeV}}$ emission. The coincidence in a typical time window of about $250 \mu\text{s}$ between the latter and the prompt signal from the e^+ gives a clear signature of an IBD event. This means that, in the time integrated events spectrum, there will be a very high peak around 2.2 MeV that integrates the same number of events expected for IBD, reduced by the efficiency of the tag. The spectral shape of this peak is due to both the energy resolution of the detector and the quenching of the gamma ray energy in the scintillator. In this work, due to lack of information, we neglect the last effect and consider the optimistic case in which the width of this peak is only due to the energy resolution.

The **superallowed CC reactions** $\nu_e + {}^{12}\text{C} \rightarrow e^- + {}^{12}\text{N}$ and $\bar{\nu}_e + {}^{12}\text{C} \rightarrow e^+ + {}^{12}\text{B}$ present physical thresholds of $E_{\nu_e} > 17.3 \text{ MeV}$ and $E_{\bar{\nu}_e} > 14.4 \text{ MeV}$ respectively. They are detectable through the prompt leptons e^- (e^+), which give a continuous spectrum. Moreover the nucleus of both reactions in the final state, ${}^{12}\text{N}$ and ${}^{12}\text{B}$, are unstable. The former will decay β^+ to ${}^{12}\text{C}$ with a half life of $\sim 11 \text{ ms}$. The latter will decay β^- to ${}^{12}\text{C}$ with a half life of $\sim 20 \text{ ms}$ [16]. The high energy positrons and electrons emitted in these beta decays can be observed, giving the possibility to tag these events. The cross sections used for the evaluation are those reported in [17].

In the NC channels all neutrino flavors are involved potentially increasing the number of signal events detected.

For the **ES on protons** channel the cross section in [18, 19] was used, with a proton strangeness of $\eta = 0.12$. However it is important to stress that the uncertainty on the number of events expected for this channel is not negligible due to the proton structure and amounts to about 20% [20]. To understand the spectral shape of this class of events it is necessary to model the quenching factor for protons in the scintillators; this accounts for the proton light output and depends on the liquid scintillator composition. A detailed description of this factor is given in the next section.

The cross section for the **superallowed NC reaction** $\nu + {}^{12}\text{C} \rightarrow \nu + {}^{12}\text{C}^*$ followed by the emission of a monochromatic γ at 15.11 MeV is reasonably well known. It was measured in KARMEN [21], confirming the correctness of the calculations as reported in [17] within an accuracy of 20%. Future measurements, most remarkably in OscSNS [22], claim the possibility of measuring more than 1,000 events in one year with a systematic estimated at 5% level or better. The prominent spectral feature of this channel can permit the identification of these events, as a sharp peak around 15 MeV, standing out from the main signal due to IBD.

The total cross section for **NC proton knockout** $\nu + {}^{12}\text{C} \rightarrow \nu + p + {}^{11}\text{B}$ has been calculated in [23], as a part of a network of reactions needed to describe the nucleosynthesis of light elements. However, the calculation of [24] finds a cross section about 30% larger, which suggests an error of at least this order. The neutrino energy has to exceed a pretty high threshold, i.e. $E > [(M_B + m_p)^2 - M_C^2] / (2M_C) \simeq 15.9 \text{ MeV}$ (where we use obvious symbols for the masses of the carbon nucleus, of the boron nucleus and of the proton). The initial neutrino energy (minus the activation energy, quantified by the threshold) is shared by the neutrino and the proton in the final state, $E + M_C \approx E' + T_p + M_B + m_p$ so that the maximum kinetic proton energy T_p^{max} is obtained when the final state neutrino is almost at rest, $E' \approx 0$. The expression for the maximum of the proton kinetic energy is

$$T_p^{\text{max}} = [(M^* - m_p)^2 - M_B^2] / (2M^*), \quad (3.1)$$

with $M^* = \sqrt{M_C^2 + 2M_C E}$. In view of the smallness of this sample of events, we adopted

a very simple procedure to describe the distribution in the kinetic energy of the proton T_p , namely, we resorted to the pure phase space, that gives $d\sigma/dT_p \propto d\Phi/dT_p \propto \sqrt{T_p}(M^* - m_p - m_B - T_p)^2$. We checked that the integral in the proton kinetic energy of this expression agrees at the level of few percent with the theoretical behaviour of the total cross sections as reported in [23].¹

In the **CC knockout proton** reaction on ^{12}C the outgoing kinetic energy is shared between the electron and the proton. The maximum kinetic proton energy T_p^{max} is obtained when the final electron is at rest. Similarly to the previous case, this is given by

$$T_p^{\text{max}} = [(M^* - m_p - m_e)^2 - M_{C11}^2] / (2M^* - 2m_e), \quad (3.2)$$

where again $M^* = \sqrt{M_C^2 + 2M_C E}$. In this case the phase space is $d\sigma/dT_p \propto d\Phi/dT_p \propto \sqrt{T_p}(M^* - m_p - m_{C11} - T_p)^2$. The theoretical cross sections reported in [23] and the value estimated from pure phase space agree at the level of $\sim 20\%$.

In the **Elastic Scattering on electrons** all the flavors participate, but the cross section is slightly different for the different flavors. The current best measurement of this interaction arises in a sample of 191 events [25, 26], and quotes 17% of total error. The error that we estimate in the standard model is instead absolutely negligible for our purposes.

Numerical formulae

Let us conclude this section by giving two numerical formulas to evaluate easily the main neutral current cross sections:

An easy-to-implement effective formula for the $\nu + ^{12}\text{C} \rightarrow \nu + ^{12}\text{C}^*$ cross section, that agrees with [17] results at better than 1% in the region below 100 MeV, is

$$\frac{1}{2}(\sigma_\nu + \sigma_{\bar{\nu}}) = \frac{G_F^2}{\pi}(E - 15.11 \text{ MeV})^2 \cdot 10^{p(E)}, \quad (3.3)$$

with $p(E) = \sum_{n=0}^3 c_n (E/100 \text{ MeV})^n$ where E is the incoming neutrino energy, and the numerical coefficients are $c_0 = -0.146$, $c_1 = -0.184$, $c_2 = -0.884$, $c_3 = +0.233$.

A simple parametrization of the cross section for the ES scattering, $\nu p \rightarrow \nu p$, assuming that the proton strangeness is $\eta = 0.12$, is simply

$$\frac{1}{2}(\sigma_\nu + \sigma_{\bar{\nu}}) = G_F^2 E^2 \cdot 10^{q(E)}, \quad (3.4)$$

where $q(E) = -0.333 - 0.16(E/100 \text{ MeV})$.

4 Description of the Ultra-pure Scintillating Detectors

We consider the ultrapure liquid scintillators detectors that are running or under construction, namely the following three: Borexino (BRX) [6] (0.3 kt of C_9H_{12}) in Gran Sasso National Laboratory, Italy, KamLAND (KAM) in Kamioka Observatory, Japan [7] (1 kt of mixture of

¹However, a word of caution is in order; while the above considerations on phase space are suggestive, they are just a reasonable way to explore of the consequences of this reaction in scintillator detectors: in fact, the distribution in T_p of [23] is not available. Certainly, it would be better to have a true calculation of the distribution in T_p of this reaction (or possibly its parameterization) along with an assessment of the theoretical error in the relevant energy range.

	a_1	a_2	$a_3[\text{MeV}^{-1}]$
BRX	0.624	-0.175	-0.154
KAM	0.581	-0.0335	-0.207
SNO+	0.629	-0.286	-0.163

Table 1. Constants appearing in the parametrized formula of the quenching function here adopted.

$C_{12}H_{20}$ (80%) and C_9H_{12} (20%)) and SNO+ (0.8 kt of $C_6H_5C_{12}H_{25}$) currently under construction in the SNOLAB facility, located approximately 2 km underground in Sudbury, Ontario, Canada [27].

We assume that the energy resolution for each detector is a Gaussian with an error described by $\sigma(E_d) = A \times \sqrt{E_d/\text{MeV}}$ and a different value of the constant A for each detector. The trigger threshold in Borexino is as low as about 200 keV, reaching full efficiency at $E_d = 250$ keV [28]. The overall light collection in Borexino is $\simeq 500$ photoelectrons (p.e.)/MeV of deposited energy. The resolution is $\simeq 5\%$ at 1 MeV (namely $A = 50$ keV). The trigger efficiency in KamLAND currently reaches 100% at 350 keV. The energy resolution of the KamLAND detector can be expressed in terms of the deposited energy as $\sim 6.9\%/\sqrt{E_d(\text{MeV})}$ (i.e., $A = 69$ keV) [9]. The energy threshold expected for SNO+ is the optimistic one of 200 keV and the energy resolution is supposed to be the same as in Borexino.

As we mentioned earlier when the detected particle is a proton, the visible energy is only a fraction of the kinetic energy T_p , as described by the ‘quenching function’. Each detector has its own quenching function, that depends on its chemical composition; for Borexino detector we consider the quenching function discussed in [20], for KamLAND the one recently discussed in [30] and finally for SNO+ the response to proton in LAB scintillator as measured in [31].

Following [29] a simple parametrization of the quenching function is

$$E_d = a_1[1 - \exp(a_2 + a_3 \cdot T_p)] \cdot T_p \quad (4.1)$$

The values for the constants a_1 , a_2 and a_3 that should be used for the different detectors are reported in Tab. 4 and the resulting functions are shown in Fig.2.

At this point, we obtain the following important conclusion:

in ultrapure scintillators, the observation of protons from the NC elastic scattering reaction allows us to observe only the high energy part of the neutrino spectra.

In fact, due to the thresholds and to the quenching, the protons below a minimum kinetic energy cannot be detected; this is 0.9 MeV for SNO+, 1.8 MeV for Kamland and 1.3 MeV for Borexino. Thus, taking into account the kinematical relation between the proton kinetic energy and the one of incoming neutrinos, we find that the elastic scattering on protons is sensitive to neutrino energies above a threshold of 22 MeV in the best situation of SNO+, it becomes 25 MeV for Borexino, and raises to 30 MeV in the case of Kamland. In view of these considerations, one concludes that the exploration of the low energy of the spectrum via neutral currents is not possible with the existing ultrapure scintillators.

5 Results

For each detection channel, we estimate the number of expected events and report them in Table 2. Moreover, we plot the energy distributions of the events, considering the specific features of the ultrapure scintillating detectors in Figure 3.

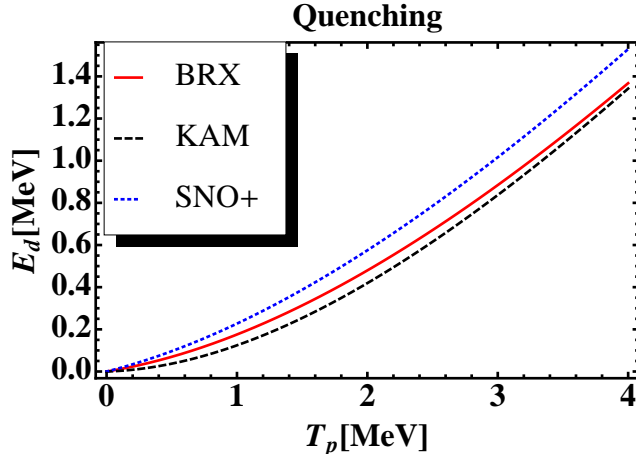


Figure 2. *Quenching functions used to convert the proton kinetic energy in the detectable energy E_d for Borexino (red line), KamLAND (black dashed line) and SNO+ (blue dotted line), respectively.*

The IBD channel (red line) starts to dominate the global signal at 5 MeV and reaches the maximum around 14 MeV. The total number of interactions expected for a supernova located at 10 kpc is of about 54 events for Borexino, 257 for Kamland and 176 for SNO+. These results are reported in the first row of Table 2. The subsequent gamma from neutron capture gives the peak at 2.2 MeV, shown by a purple line. The efficiency of the neutron tag is $(85\pm 1)\%$ in Borexino (see [39]), $(78\pm 2)\%$ in KamLAND (see [7]) and also in SNO+. The condition for a successful IBD tag [39] is that no more than one interaction occurs during the time between the IBD interaction and the neutron capture inside a specific volume, namely

$$R_{IBD} \times \Delta t \Delta V \rho \leq 1 \quad (5.1)$$

where R_{IBD} is the rate of IBD events per second and per unit mass, Δt is the temporal window of the tag, that we assume to be $\Delta t = 2\tau = 512\mu s$, ΔV is the volume of a sphere with 1 meter of radius, ρ is the density of the scintillator. This is related to the detector mass and to the distance of the supernova by

$$R_{IBD} = \frac{256.5}{T} \cdot \left(\frac{10\text{kpc}}{D}\right)^2 \cdot \left(\frac{M}{1\text{kton}}\right), \quad (5.2)$$

where M is the mass of the detector, D is the distance of the SN and T is the duration of the emission. For example to allow the IBD tag in a detector with the density of Borexino and 1 kton of mass, considering that 50% of the total emission is expected during the first second [11], then the minimum distance of a SN is $D \geq 0.16$ kpc, that is not a severe limitation.²

Let us discuss now the NC elastic proton scattering. This channel dominates the low energy part of the spectrum, represented with the blue line in Figure 3, even if as discussed previously, this reaction probes only the high energy part of the supernova neutrinos. It is

²If instead, a similar detector but with a 50 kton mass is considered the distance becomes $D \geq 1.13$ kpc, that includes several known potential Core-Collapse SNe as Betelgeuse and VY Canis Majoris [43].

Channel	Color code	Signal	BRX	KAM	SNO+
$\bar{\nu}_e + p \rightarrow n + e^+$	red	e^+	54.1 (49.6)	256.5 (235.3)	175.8 (161.2)
$n + p \rightarrow D + \gamma_{2.2 \text{ MeV}}$	purple	γ	46.0 (42.1)	200.1(183.5)	137.1 (125.8)
$\nu + p \rightarrow \nu + p$	blue	p	12.7 (3.8)	29.0 (6.2)	74.9 (29.2)
$\nu + {}^{12}\text{C} \rightarrow \nu + {}^{12}\text{C}^*$	orange	γ	4.7 (2.1)	15.0 (6.7)	12.3 (5.5)
$\nu + e^- \rightarrow \nu + e^-$	green	e^-	4.4 (4.5)	14.8 (15.5)	12.0 (12.4)
$\nu_e + {}^{12}\text{C} \rightarrow e^- + {}^{12}\text{N}$	magenta	e^-	2.0 (0.7)	6.4 (2.1)	5.3 (1.7)
$\bar{\nu}_e + {}^{12}\text{C} \rightarrow e^+ + {}^{12}\text{B}$	black thin	e^+	1.2 (0.8)	3.7 (2.6)	3.0 (2.1)
$\nu + {}^{12}\text{C} \rightarrow \nu + p + {}^{11}\text{B}$	yellow	p	0.7 (0.2)	2.4 (0.6)	2.1 (0.6)
$\nu_e + {}^{12}\text{C} \rightarrow e^- + p + {}^{11}\text{C}$	red dashed	p	0.5 (0.1)	1.5 (0.3)	1.3 (0.2)

Table 2. Summary table for all the number of events from the various interaction channels. The result are given for the emission model where the energy of non-electronic components is 30% bigger than the one of $\bar{\nu}_e$; in brackets, we indicate the correspondent values assuming that the energies of $\bar{\nu}_e$ and ν_x are the same. The color code (2nd colum) refers to the lines of Figure 3.

evident from Table 2 and Fig. 3 that the event spectrum depends strongly on the quenching of the proton signal. The detector threshold used in the case of KamLAND is an optimistic value, since we assumed a threshold of 350 keV, lower than the one that can be obtained with the current radioactivity level, i.e., 600 keV [40]. If this higher threshold is assumed the ES with protons on KamLAND gives only 17 signal events.

It is important to remark that the number of events due to this channel is also very sensitive to the SN emission parameters; in fact, as discussed in the end of the previous section, this interaction is sensitive only to the high energy tail of the SN neutrinos spectra. In particular, the average energy of the different neutrino flavors have gradually been changing in recent years, moving toward lower mean values [41] and toward minor differences between the average energies of the different components [13, 42]. For comparison we have considered the new paradigm of emission, where the average energy of non-electronic flavors is the same as of the electronic antineutrinos, namely $\langle E_x \rangle = 12 \text{ MeV}$ [13, 41] and have investigated the two different cases to outline the impact on this and the other NC process. As shown by the values in brackets in Table 2, the expectations in this case are quite meager.

The NC neutral current reaction $\nu + {}^{12}\text{C} \rightarrow \nu + {}^{12}\text{C}^*$ followed by the emission of a monochromatic γ is shown in orange in Figure 3. This channel does not require the low energy threshold and the efficiency for its detection is taken 100% for all the detectors considered. However, the possibility of a successful identification is affected by the quality of the energy resolution of the detector and by the effectiveness to tag the IBD signal. These events can be observed if the IBD events are identified through the correlated neutron capture signal, since they are expected to occur in the same energy region. With the assumed energy resolutions we have that this neutral current reaction can be observed in the energy range (14-16) MeV. For Borexino, the number of events due to the IBD signal in the same range is 5.7; thus, more than the 50% of the total signal collected in this energy window is due to the IBD channel, while for KamLAND and SNO+ the IBD signal is 26.9 and 18.4, representing about 60% of the total one. In the case of Borexino, if the tagging efficiency is of 85% as assumed in the plot, we expect only 1 event due to IBD not identified, so the uncertainty on the $\gamma_{15.11\text{MeV}}$ signal is reduced to 14%.

The ESe involves all the flavors of neutrinos and we expect to collect about 4 events for Borexino, 15 for KamLAND and 12 for SNO+. Their spectrum is reported with a dark

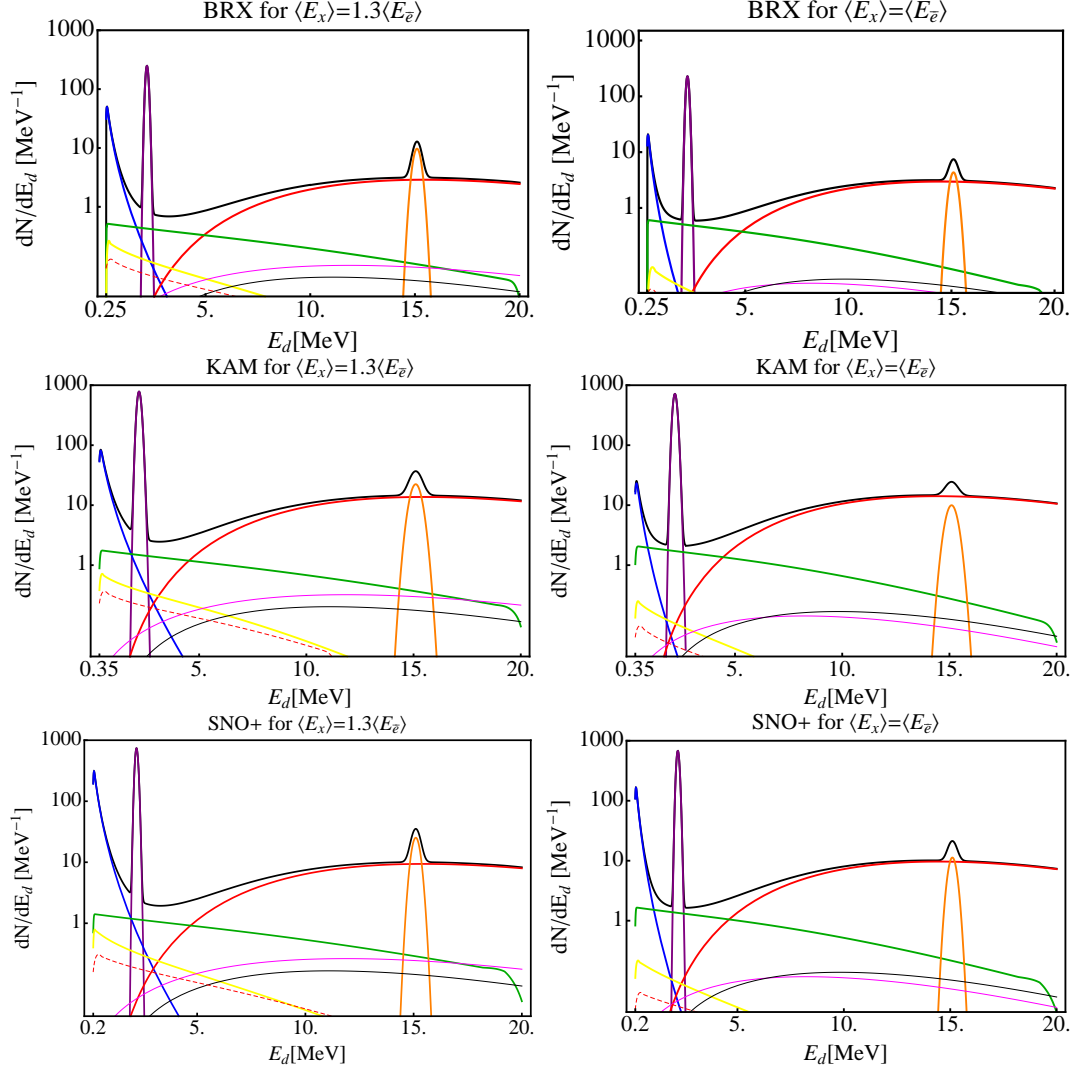


Figure 3. Theoretical event spectrum in the detectable energy E_d in ultrapure scintillators for a Supernova exploding at 10 kpc. The top panels refer to Borexino detector, the bottom panels to SNO+, those in the middle to KamLAND. On the left panels, the expectations for the emission model where energy of non-electronic component is 30% higher than the one of $\bar{\nu}_e$; on the right panels, the corresponding expectations for the case when the non-electronic components and the $\bar{\nu}_e$ have the same average energy. See Table 2 and the text for the explanation of the individual lines.

green line in the spectra of Figure 3, and dominates in the energy region between the ES on protons and the IBD signals. As we mentioned the cross section for the different flavors are slightly different; the ν_e contribution produces half of the events.

The rest of the detection channels have a low signal. All of them show a continuous spectrum, being from e^- , e^+ or protons. The two CC superallowed reactions are indicated by a magenta line for the ^{12}N final state nucleus and by a black thin line for the ^{12}B one. The decay products of the unstable nucleus are not considered in this plot. For both knockout channels, besides the high energy thresholds, the quenching has to be considered, so the total number of events collected for them is pretty small. The one due to NC is shown in yellow, while the one due to CC is shown with the dashed red line.

6 Conclusions

In this paper, we have obtained and discussed the spectrum of supernova neutrino events in ultrapure scintillators for a supernova exploding at 10 kpc from the Earth. We have examined the capability to distinguish the various detection channels and we have quantified the uncertainties in this type of detectors.

As discussed in the introduction, a major reason of specific interest for a future supernova is the possibility to observe neutral current interactions of neutrinos. We have investigated the three possible reactions of detection in ultrapure scintillators, namely: 1) the elastic scattering with protons, 2) the 15.11 MeV γ de-excitation line, 3) the proton knockout channel. Our conclusions are as follows:

The first reaction is characterized by the larger number of expected events in all the detectors; however the number of detectable events is strongly limited by the energy thresholds. The uncertainty on the total number of elastic scattering on protons, due to the proton structure, amounts to the 20%; moreover in the same energy region where this reaction can be observed there are also the indistinguishable events due to the elastic scattering with electrons and those due to NC and CC proton knockout. In other words, all we can observe is the total number of events collected in the energy region from the detector threshold to the threshold of the IBD signal, about 1.8 MeV. In this detection window, we have found that a fraction of 8% (Borexino), the 7% (KamLAND), the 4% (SNO+) of the signal is due to the other channels and this uncertainty is small but irreducible. We have also seen that, in the case that the energy of non-electronic neutrinos is low, the number of events due to this reaction is too small to permit the investigation of the ν_x spectrum at the level discussed in [9].

The gamma line due to neutrino-induced ^{12}C de-excitation is in principle easier, giving a signal at a high energies; its detection does not require the extreme performances at very low energies are not needed. However, in the same region of the spectrum where this line is visible we will have also positrons due to IBD reaction; thus, the efficiency to tag the concomitant neutron will be of crucial importance to identify cleanly a sample of this NC reaction. While this concern is not a severe issue for the type of detectors we have considered in this work, it is much more relevant for future scintillators with a much larger mass and limited performances at low energies.

Finally, we have shown that the proton knockout will give a comparably small number of NC events.

References

- [1] K. Hirata, et al., *Observation of a Neutrino Burst from the Supernova SN 1987a*, *Phys. Rev. Lett.* **58** (1987) 1490.
- [2] R. M. Bionta, et al., *Observation of a Neutrino Burst in Coincidence with Supernova SN 1987a in the Large Magellanic Cloud*, *Phys. Rev. Lett.* **58** (1987) 1494.
- [3] E. N. Alekseev, et al., *Possible Detection of a Neutrino Signal on 23 February 1987 at the Baksan Underground Scintillation Telescope of the Institute of Nuclear Research*, *JETP Lett.* **45** (1987) 589.
- [4] M. Ikeda, et al. [Super-Kamiokande Collaboration], *Search for Supernova Neutrino Bursts at Super-Kamiokande*, *Astrophys. J.* **669** (2007) 519 [arXiv:0706.2283 [astro-ph]].

- [5] R. Abbasi, et al. [IceCube Collaboration], *IceCube Sensitivity for Low-Energy Neutrinos from Nearby Supernovae*, *Astron. Astrophys.* **535** (2011) A109 [arXiv:1108.0171 [astro-ph.HE]].
- [6] G. Alimonti, et al. [Borexino Collaboration], *The Borexino detector at the Laboratori Nazionali del Gran Sasso*, *Nucl. Instrum. Meth.* **A 600** (2009) 568
- [7] K. Eguchi, et al. [KamLAND Collaboration], *First results from KamLAND: Evidence for reactor anti-neutrino disappearance* *Phys. Rev. Lett.* **90** (2003) 021802
- [8] J. F. Beacom, W. M. Farr and P. Vogel, *Detection of supernova neutrinos by neutrino proton elastic scattering*, *Phys. Rev. D* **66** (2002) 033001
- [9] B. Dasgupta and J. F. Beacom, *Reconstruction of supernova ν_μ , ν_τ , anti- ν_μ , and anti- ν_τ neutrino spectra at scintillator detectors*, *Phys. Rev. D* **83** (2011) 113006
- [10] T. J. Loredo and D. Q. Lamb, *Bayesian analysis of neutrinos observed from supernova SN-1987A*, *Phys. Rev. D* **65** (2002) 063002 [astro-ph/0107260].
- [11] G. Pagliaroli, F. Vissani, M. L. Costantini and A. Ianni, *Improved analysis of SN1987A antineutrino events*, *Astropart. Phys.* **31** (2009) 163 [arXiv:0810.0466 [astro-ph]].
- [12] M. T. Keil, G. G. Raffelt and H. -T. Janka, *Monte Carlo study of supernova neutrino spectra formation*, *Astrophys. J.* **590** (2003) 971 [astro-ph/0208035].
- [13] I. Tamborra, B. Muller, L. Hudepohl, H. -T. Janka and G. Raffelt, *High-resolution supernova neutrino spectra represented by a simple fit*, *Phys. Rev. D* **86** (2012) 125031 [arXiv:1211.3920 [astro-ph.SR]].
- [14] B. Mueller and H. -T. Janka, arXiv:1402.3415 [astro-ph.SR].
- [15] A. Strumia, F. Vissani, *Precise quasielastic neutrino/nucleon cross-section* *Phys. Lett.* **B 564** (2003) 42.
- [16] F. Ajzenberg-Selove, *Energy levels of light nuclei $A = 11-12$* , *Nucl. Phys.* **A 506** (1990) 1
- [17] M. Fukugita, Y. Kohyama, K. Kubodera, *Neutrino Reaction Cross-Sections on C-12 Target* *Phys. Lett.* **B 212** (1988) 139.
- [18] L.A. Ahrens, et al. [BNL 734] *Measurement of Neutrino - Proton and anti-neutrino - Proton Elastic Scattering*, *Phys. Rev. D* **35** (1987) 785.
- [19] <http://theory.lngs.infn.it/astroparticle/sn.html>
- [20] G. Pagliaroli, C. Lujan-Peschard, M. Mitra and F. Vissani, *Using Low-Energy Neutrinos from Pion Decay at Rest to Probe the Proton Strangeness*, *Phys. Rev. Lett.* **111** (2013) 022001.
- [21] B. E. Bodmann, et al. [KARMEN. Collaboration], *Neutrino interactions with carbon: Recent measurements and a new test of electron-neutrino, anti-muon-neutrino universality*, *Phys. Lett.* **B 332** (1994) 251.
- [22] H. Ray [OscSNS Collaboration], *OscSNS: Precision Neutrino Measurements at the Spallation Neutron Source*, *J. Phys. Conf. Ser.* **136** (2008) 022029 [arXiv:0810.3175 [hep-ex]].
- [23] T. Yoshida, et al. *Neutrino-Nucleus Reaction Cross Sections for Light Element Synthesis in Supernova Explosions* *Astrophys. J.* **686** (2008) 448
- [24] A. Heger, E. Kolbe, W. C. Haxton, K. Langanke, G. Martinez-Pinedo and S. E. Woosley, *Neutrino nucleosynthesis*, *Phys. Lett.* **B 606** (2005) 258
- [25] L. B. Auerbach, et al., *Measurement of electron - neutrino - electron elastic scattering*, *Phys. Rev. D* **63** (2001) 112001.
- [26] R. C. Allen, et al., *Study of electron-neutrino electron elastic scattering at LAMPF* *Phys. Rev. D* **47** (1992) 11.

- [27] H. M. O’Keeffe, E. O’Sullivan, M. C. Chen, *Scintillation decay time and pulse shape discrimination in oxygenated and deoxygenated solutions of linear alkylbenzene for the SNO+ experiment*, *Nucl. Instrum. Meth.* **A 640** (2011) 119.
- [28] C. Arpesella et al. [Borexino Collaboration], *Direct Measurement of the Be-7 Solar Neutrino Flux with 192 Days of Borexino Data*, *Phys. Rev. Lett.* **101** (2008) 091302.
- [29] R. Madey, et al., *Nucl. Instrum. Meth.* **151** (1978) 445.
- [30] S. Yoshida et al. *Light output response of KamLAND liquid scintillator for protons and 12 C nuclei*, *Nucl. Instrum. Meth.* **A 622** (2010) 574.
- [31] B. von Krosigk, L. Neumann, R. Nolte, S. Rottger and K. Zuber, *Measurement of the proton light response of various LAB based scintillators and its implication for supernova neutrino detection via neutrino-proton scattering*, arXiv:1301.6403 [astro-ph.IM].
- [32] D. K. Nadyozhin, *The neutrino radiation for the hot neutron star formation and the envelope outburst problem*, *Astrophys. Space Sci.* **53** (1978) 131.
- [33] H. A. Bethe, J. R. Wilson, *Revival of a stalled supernova shock by neutrino heating*, *Astrophys. J.* **295** (1985) 14.
- [34] H. Duan, G. M. Fuller and Y. -Z. Qian, *Collective Neutrino Oscillations*, *Ann. Rev. Nucl. Part. Sci.* **60** (2010) 569 [arXiv:1001.2799 [hep-ph]].
- [35] G. Badino, et al., *The 90 ton liquid scintillator detector in the mont blanc laboratory*, *Nuovo Cimento C* **7** (1984) 573.
- [36] N. Yu. Agafonova, et al., *Study of the effect of neutrino oscillations on the supernova neutrino signal in the LVD detector*, *Astropart. Phys.* **27** (2007) 254.
- [37] P. Antonioli, W. Fulgione, P. Galeotti and L. Panaro *Simulation of low-energy neutrino interactions in liquid scintillation counters*, *Nucl. Instrum. Meth.* **A 309** (1991) 569.
- [38] T. Totani, K. Sato, H. E. Dalhed and J. R. Wilson, *Future detection of supernova neutrino burst and explosion mechanism*, *Astrophys. J.* **496** (1998) 216 [astro-ph/9710203].
- [39] G. Bellini, et al. [Borexino Collaboration], *Observation of Geo-Neutrinos*, *Phys. Lett.* **B 687** (2010) 299.
- [40] K. Tolich [KamLAND Collaboration], *Supernova detection with KamLAND* *Nucl. Phys. Proc. Suppl.* **221** (2011) 355.
- [41] H. -T. Janka, *Explosion Mechanisms of Core-Collapse Supernovae*, *Ann. Rev. Nucl. Part. Sci.* **62** (2012) 407 [arXiv:1206.2503 [astro-ph.SR]].
- [42] C. D. Ott, et al. *General-Relativistic Simulations of Three-Dimensional Core-Collapse Supernovae*, *Astrophys. J.* **768** (2013) 115 [arXiv:1210.6674 [astro-ph.HE]].
- [43] N. Smith, K. H. Hinkle, and N. Ryde, *Red Supergiants as Potential Type II_n Supernova Progenitors: Spatially Resolved 4.6 μ m CO Emission Around VY CMa and Betelgeuse*, *The Astronomical Journal* **137** (2009) 3558.